Phase Behavior and Hydrogen Bonding in Ternary Polymer Blends of Phenolic Resin/Poly(ethylene oxide)/Poly(ϵ-caprolactone)

Shiao-Wei Kuo, Chen-Lung Lin, and Feng-Chih Chang*

Institute of Applied Chemistry, National Chiao Tung University, Hsinchu, Taiwan

Received July 17, 2001; Revised Manuscript Received October 12, 2001

ABSTRACT: The phase behavior and hydrogen bonding in ternary polymer blends of phenolic resin, poly(ethylene oxide) (PEO), and poly(ϵ-caprolactone) (PCL) were investigated by using differential scanning calorimetry (DSC) and Fourier transform infrared spectroscopy (FTIR). Although all three binary blends are respective miscible, there exists a closed immiscibility loop in the phase diagram due to the so-called "$\Delta\chi$" and "ΔK" effects in this hydrogen-bonded ternary polymer system. The interassociation equilibrium constant based on the Painter−Coleman association model between phenolic resin and PEO can be indirectly calculated from the fraction of hydrogen-bonded carbonyl groups. Quantitative analyses show that the hydroxyl−ether interassociation is more favorable than the hydroxyl−carbonyl interassociation at room temperature. The interaction energy density value of $B_{PEO/PCL} = -2.85$ cal/cm^3 was obtained by comparing the theoretically predicted phase diagram with experimental data.

Introduction

The phase behavior and miscibility of ternary polymer blends have received great attention in polymer science due to its significant industrial importance. Many prior studies of ternary polymer blends have paid their attention primarily to two or three pairs of miscible polymers. When all three binary pairs (B−A, B−C, and A−C) are individually miscible, a completely homogeneous or a closed immiscibility loop phase diagram has been observed.[1] The phase separation is caused by the difference in the interaction energy of the binary system, the so-called "$\Delta\chi$" and the "ΔK" effects in ternary polymer blends such as phenoxy/poly(methyl methacrylate) (PMMA)/PEO,[2] poly(vinylphenol) (PVPh)/poly(vinyl acetate) (PVAc)/PEO,[3] and poly(styrene-*co*-acrylic acid)/PMMA/PEO[4] blend systems. In the case of only two pairwise miscible polymers (B−A, B−C) in which the third pair (A−C) is immiscible, a large amount of third polymer (B) can occasionally make a homogeneous ternary polymer blend such as PVPh/PMMA/poly(ethyl methacrylate) (PEMA)[5] or PVPh/PVAc/poly(styrene-*co*-methyl methacrylate)[6] blend systems which are analogous to introduction of a good solvent to the mix of two immiscible polymers. We have developed some compatibilizers (B) into immiscible binary homopolymers A and C.[7−9] These compatibilizers are able to obtain finer dispersion and to stabilize the morphology due to low interfacial tension.

In our previous study, we have found that the binary pairs of phenolic/PCL[10] and phenolic/PEO[11] are totally miscible over the entire compositions in the amorphous phase due to interassociation hydrogen bonding between the hydroxyl group of phenolic and the carbonyl group of PCL and the ether group of PEO, respectively. In the present study, we have investigated the phase behavior and hydrogen bonding in ternary blends of phenolic/PEO/PCL. At first glance, this ternary blend seems complicated to be analyzed by DSC due to the closeness of the glass transition temperature (T_g) of phenolic (66 °C), melting temperature (T_m) of PEO (70 °C), and melting temperature of PCL (60 °C). Furthermore, the glass transition temperatures of PEO and PCL are also close to each other (≒−60 °C). However, for a multifunctional polymer blend system, the interassociation equilibrium constant of individual binary miscible pairs should be different. Using the concept of competing equilibrium constants, we are able to identify which phase transition is caused by the hydroxyl−ether or the hydroxyl−carbonyl interassociation.

By Fourier transform infrared (FTIR) spectroscopy, the carbonyl, hydroxyl, and ether vibration have been proved to be the excellent tool to detect these molecular interactions.[12−15] This tool can be used to study the mechanism of interpolymer miscibility through the formation of different type hydrogen bonds both qualitatively and quantitatively. According to our previous study,[10] the interassociation equilibrium constant (K_A) between hydroxyl group of phenolic resin and carbonyl group of PCL was calculated at different temperatures and compositions based on the fraction of hydrogen-bonded carbonyl group. However, the interassociation equilibrium constant between the phenolic hydroxyl group and the PEO ether group is not able to determine directly because no carbonyl group is available to be used as a measure of the fraction of the hydrogen-bonded group from IR analysis in this binary blend. The ether stretching mode near 1100−1200 cm^{-1} is a highly coupled mode that is conformationally sensitive and cannot be readily decomposed into two peaks, with areas corresponding to the free and the hydrogen-bonded ether absorptions. In general, the interassociation equilibrium constant between phenolic hydroxyl group and PEO ether group is calculated from model compounds[16] by using classical Coggeshall and Saier (C&S)[17] methodology. However, the interassociation equilibrium constant obtained from model compounds is not exactly the same as that from the true polymer blend due to the

* To whom correspondence should be addressed: e-mail changfc@cc.nctu.edu.tw; Tel 886-3-5712121, ext 56502; Fax 886-3-5723764.

10.1021/ma011255f CCC: $22.00
Published on Web 12/01/2001

Chart 1

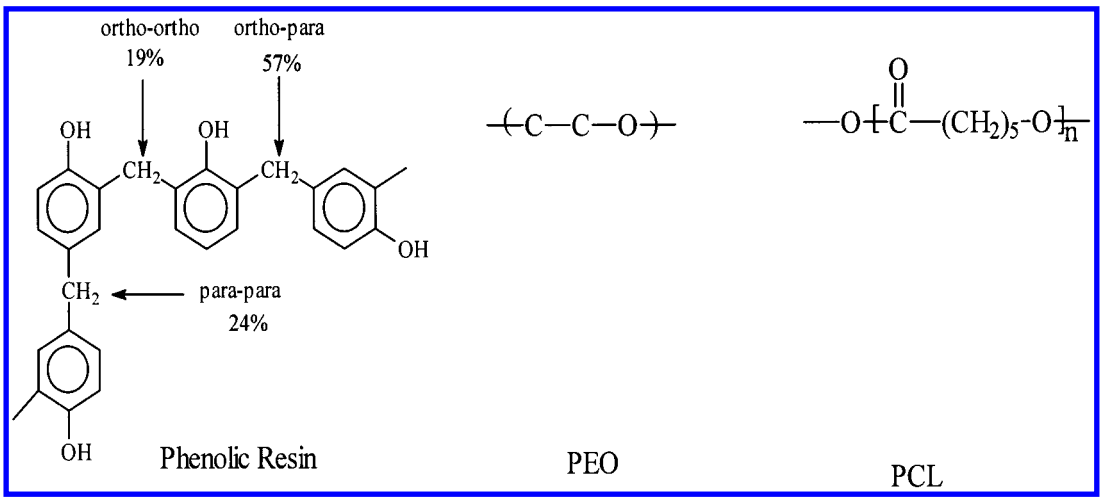

intramolecular screening and functional group accessibility effects[18−23] as well as the chain stiffness and connectivity in the miscible polymer blend. In the present study, the K_A value is determined indirectly from a least-squares fitting procedure of the experimental fraction of hydrogen-bonded carbonyl group in the ternary polymer blend. Notably, we need to ensure the ternary compositions rich in phenolic rich that form single phase because the K_A value will be difference between the miscible and immiscible phase. We also need to emphasize that although the self-association equilibrium constants (K_2 and K_B) are determined from the model compounds, the relative magnitudes of the inter- and self-association are more important than their individual absolute values in determining the contribution of the free energy of mixing. We found that the interassociation equilibrium constant of hydroxyl−ether is higher than the interassociations equilibrium constant of the hydroxyl−carbonyl at room temperature from the least-squares fitting procedure. Furthermore, we have investigated the phase boundary of ternary phenolic/PEO/PCL blends and determined the interaction energy density $B_{PEO/PCL}$ by using the experimental data with theoretical phase diagram. The negative value of $B_{PEO/PCL}$ indicates that the PEO/PCL is a miscible blend in the amorphous phase.

Experiment

Samples. The phenolic was synthesized with sulfuric acid via a condensation reaction with average molecular weights M_n = 500 and M_w = 1200. The chemical structure of this Novolac-type phenolic resin contains 0.15 wt % free phenol and consists of phenol rings bridge-linked randomly by methylene groups with 19% ortho−ortho, 57% ortho−para, and 24% para−para methylene bridges was determined by the solution ^{13}C NMR spectrum.[24] The phenolic resin does not contain any reactive methylol group which is capable of causing cross-linking on heating. The poly(ethylene oxide) (PEO) with M_n = 20 000 was obtained from Aldrich Co. The PCL used in this study is the TONE Polymer P-787 purchased from Union Carbide Corp. with M_n = 80 000. The chemical structures of phenolic resin, PEO, and PCL are illustrated in Chart 1.

Blend Preparations. Blends of various ternary phenolic/PEO/PCL blend compositions were prepared by solution casting. Tetrahydrofuran solution containing 5 wt % polymer mixture was stirred for 6−8 h and cast on a Teflon dish. The solution was allowed to evaporate slowly at room temperature for 1 day. The blend films were then dried at 50 °C for 2 days.

Characterizations. 1. Differential Scanning Calorimetry. Thermal analysis was carried out on a DSC instrument from DuPont (model 910 DSC-9000 controller) with a scan rate of 20 °C/min and temperature range of 30−100 °C. The measurement was made using a 5−10 mg sample on a DSC sample cell after the sample was quickly cooled to −100 °C from the melt of the first scan. The glass transition temperature was obtained as the inflection point of the jump heat capacity with scan rate of 20 °C/min and temperature range of −100 to 100 °C.

2. Infrared Spectroscopy. Infrared spectra of polymer blend films were determined by using the conventional NaCl disk method. The THF solution containing the blend was cast onto a NaCl disk and dried under condition similar to those used in the bulk preparation. The film used in this study was thin enough to obey the Beer−Lambert law. FTIR measurement was recorded on a Nicolet Avatar 320 FT-IR spectrophotometer, and 32 scans were collected with a spectral resolution of 1 cm^{-1}. Owing to that fact that the sample containing hydroxyl groups is water-sensitive, a pure nitrogen flow was used to purge the IR optical box in order to maintain dry sample films.

Results and Discussion

We have reported that phenolic is totally miscible with PEO and PCL in the amorphous phase due to the interassociation hydrogen bonding between the hydroxyl group of the phenolic and the carbonyl group of the PCL or the ether group of the PEO. In general, the DSC analysis is one of the convenient methods to determine the miscibility in polymer blends. The glass transition temperature of these pure polymers used in this study, phenolic, PEO, and PCL are 66, −60, and −60 °C, respectively. Figure 1 shows the conventional second run DSC thermograms of the phenolic/PEO/PCL ternary blend containing a constant composition (80 wt %) of phenolic resin and with various PEO/PCL ratios (80:20, 60:40, 50:50, 40:60, and 20:80), revealing that essential all these phenolic/PEO/PCL ternary blends possess single T_g. A single T_g strongly suggests that these blends are fully miscible with a homogeneous amorphous phase. Meanwhile, the melting temperatures of PEO and PCL are both missing, an indication of no crystallization of the blend from these two crystallizable polymers at the higher phenolic resin compositions (80 wt %). Figure 2 shows infrared spectra recorded at room temperature in the hydroxyl (a), carbonyl (b), and ether (c) vibration region for a series of ternary blends containing a constant 80 wt % phenolic

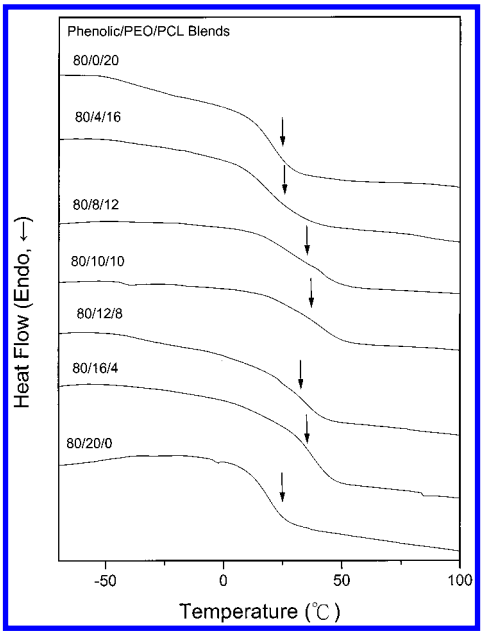

Figure 1. DSC thermograms of ternary blend of phenolic/PEO/PCL containing a constant composition (80 wt %) of phenolic resin.

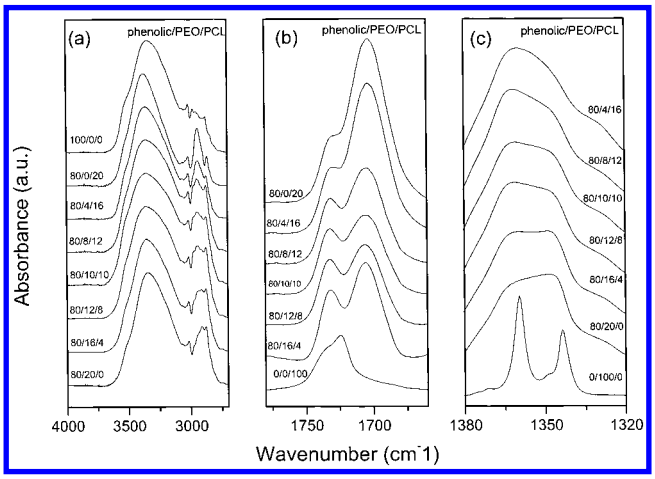

Figure 2. Infrared spectra of ternary blend of phenolic/PEO/PCL containing a constant composition (80 wt %) of phenolic resin at room temperature in the hydroxyl stretching region (a), carbonyl stretching region (b), and ether region (c).

resin. As shown in Figure 2a, the pure phenolic resin exhibits two bands in the hydroxyl stretching region of the infrared spectrum. The free hydroxyl group absorption is located at 3525 cm^{-1}, while the hydrogen-bonded hydroxyl gives a broad absorption at 3350 cm^{-1} due to wide distribution of hydrogen-bonded hydroxyl groups. In the phenolic/PCL = 80/20 binary blend, the hydrogen-bonded hydroxyl group shifts to 3370 cm^{-1}, reflecting the new distribution of hydrogen bonds between the hydroxyl−hydroxyl and the hydroxyl−carbonyl specific interactions. Furthermore, the band at 3370 cm^{-1} is shifted to 3345 cm^{-1}, a lower wavenumber, for blends with increasing PEO/PCL ratios. This change has come from the switch from the intermolecular hydroxyl−carbonyl bond to the intermolecular hydroxyl−ether bond, indicating that there is hydrogen-bonding interaction between the PEO ether group and the hydroxyl group of phenolic resin. It also reveals that the hydroxyl−ether interaction predominates in these ternary blends, so that it is reasonable to assign the band at 3345 cm^{-1} as the hydroxyl group bonded to the ether group. Coleman et al.[25] employed the frequency difference ($\Delta\nu$) between the hydrogen-bonded hydroxyl absorption and the free hydroxyl absorption in determining the relative strength of different intermolecular interactions. A $\Delta\nu$ = 185 cm^{-1} for phenolic/PEO is obtained which is stronger than that of the phenolic/PCL ($\Delta\nu$ = 155 cm^{-1}), indicating that the hydroxyl−ether interassociation is more favorable than the hydroxyl−carbonyl interassociation.

Table 1. Curve-Fitting Results of the Phenolic/PEO/PCL Ternary Blends at Room Temperature

phenolic/PEO/PC (wt %)	free C=O			H-bonded C=O			
	ν, cm^{-1}	$W_{1/2}$, cm^{-1}	A_f %	ν, cm^{-1}	$W_{1/2}$, cm^{-1}	A_b%	fb[a] (%)
80/0/20	1733.4	13.5	9.80	1703.0	28.1	90.20	85.98
80/4/16	1733.8	12.9	11.93	1702.9	29.6	88.07	83.11
80/8/12	1733.9	13.5	19.03	1705.0	29.5	80.97	73.93
80/10/10	1734.4	14.2	21.64	1705.7	31.2	78.36	70.70
80/12/8	1734.2	14.7	26.22	1705.6	27.8	73.78	65.22
80/16/4	1732.8	13.6	27.80	1705.3	23.3	72.20	63.38
65/0/35	1733.4	13.5	88.20	1703.0	28.1	11.80	83.28
65/7/28	1733.6	14.9	77.74	1705.1	27.1	22.26	69.95
65/14/21	1733.9	15.9	74.27	1704.5	26.9	25.73	65.81
65/17.5/17.5	1733.3	13.7	66.09	1705.7	24.0	28.06	56.51
65/21/14	1732.9	14.6	69.13	1705.5	24.3	30.87	59.89
65/28/7	1732.4	14.9	71.94	1704.9	26.9	33.91	63.08
50/10/40	1734.5	17.4	36.73	1705.9	29.4	63.27	53.45
50/20/30	1734.4	18.0	50.93	1706.9	27.5	49.07	39.11
50/25/25	1734.2	17.9	55.49	1707.3	26.2	44.51	34.84
50/30/20	1734.2	18.5	59.86	1707.3	25.6	40.14	30.89

[a] fb = fraction of hydrogen bonding.

Figure 2b shows the infrared spectra of the carbonyl stretching measured at room temperature ranging from 1650 to 1780 cm^{-1} for these ternary blends. The carbonyl stretching for the pure PCL is split into two bands, absorptions by the amorphous and the crystalline conformations at 1734 and 1724 cm^{-1}, respectively. This crystalline conformation at 1724 cm^{-1} disappear over the entire ternary blend compositions containing a fixed phenolic content of 80 wt %. Another band appearing at approximately 1703 cm^{-1} is assigned as the PCL carbonyl group that is hydrogen bonded to the phenolic hydroxyl group. The carbonyl stretching frequency splits into only two bands at 1734 and 1703 cm^{-1}, corresponding to the free and the hydrogen-bonded carbonyl groups, which can be fitted well to the Gaussian function. The fraction of the hydrogen-bonded carbonyl group can be calculated by using a appropriate absorptivity ratio ($a_R = a_{HB}/a_F$ = 1.5) that has also been intensively discussed in our previous study.[26] The results from curve fitting are summarized in Table 1. The hydrogen-bonded fraction of the carbonyl group decrease with the increase the relative ratio of the PEO to PCL. In other words, the PCL carbonyl competes with the ether oxygen of PEO to form a hydrogen bond with the hydroxyl group of the phenolic resin. Table 1 shows that the fraction of hydrogen-bonded carbonyl groups decreases with increasing the relative ratio of PEO to PCL. This result implies that the interassociation equilibrium constant of hydroxyl−ether is greater than the interassociations equilibrium constant of hydroxyl−carbonyl at room temperature. In our previous study,[27] we have used three competing functional groups to predict the fraction of hydrogen-bonded carbonyl group. According to the Painter−Coleman association model, we designate B, C, and A as phenolic resin, PCL, and PEO, respectively, and K_2, K_B, K_C, and K_A as their

Table 2. Summary of the Self-Association and Interassociation Equilibrium Constants and Thermodynamic Parameter of Phenolic/PEO/PCL Ternary Blends at Room Temperature

polymer	molar volume (mL/mol)	mol wt (g/mol)	solubility parameter $(cal/mL)^{0.5}$	self-association equilibrium constant		interassociation equilibrium constant	
				K_2	K_B	K_A	K_C
phenolic	84	105	12.05	23.3	52.3		
PEO	38.10	44.06	9.40			264.7	
PCL	102.1	114.1	9.21				116.8

corresponding association equilibrium constants.

$$B_1 + B_1 \overset{K_2}{\longleftrightarrow} B_2 \quad (1)$$

$$B_h + B_1 \overset{K_B}{\longleftrightarrow} B_{h+1} (h \geq 2) \quad (2)$$

$$B_h + C_1 \overset{K_C}{\longleftrightarrow} B_h C \quad (3)$$

$$B_h + A_1 \overset{K_A}{\longleftrightarrow} B_h A \quad (4)$$

These four equilibrium constants can be expressed as follows in terms of volume fractions

$$\Phi_B = \Phi_{B1}\Gamma_2\left[1 + \frac{K_A\Phi_{A1}}{r_A} + \frac{K_C\Phi_{C1}}{r_C}\right] \quad (5)$$

$$\Phi_A = \Phi_{A1}[1 + K_A\Phi_{B1}\Gamma_1] \quad (6)$$

$$\Phi_C = \Phi_{C1}[1 + K_C\Phi_{B1}\Gamma_1] \quad (7)$$

where

$$\Gamma_1 = \left(1 - \frac{K_2}{K_B}\right) + \frac{K_2}{K_B}\left(\frac{1}{1 - K_B\Phi_{B1}}\right) \quad (8)$$

$$\Gamma_2 = \left(1 - \frac{K_2}{K_B}\right) + \frac{K_2}{K_B}\left(\frac{1}{(1 - K_B\Phi_{B1})^2}\right) \quad (9)$$

Φ_B, Φ_A, and Φ_C are the volume fractions of repeat units in the blend, Φ_{B1}, Φ_{A1}, and Φ_{C1} are the volume fractions of isolated units in the blend, and $r_A = V_A/V_B$ and $r_C = V_C/V_B$ are the ratios of segmental molar volumes.

The self-association values of phenolic resin ($K_2 = 23.3$ and $K_B = 52.3$) and the interassociation between phenolic resin and PCL ($K_C = 116.8$) have been determined in our previous study.[9] The interassociation constant K_A value is determined indirectly from a least-squares fitting procedure of the fraction of hydrogen-bonded carbonyl group experimentally obtained in this ternary polymer blend. If these equilibrium constant (K_2, K_B, K_C), segment molar volume, and the fraction of hydrogen-bonded carbonyl group are known, the K_A value can be calculated from eqs 5−9 by using a least-squares fit based on the fraction of hydrogen-bonded carbonyl group experimentally obtained. We obtained a value for $K_A = 264.7$ at room temperature, implying that the interassociation equilibrium constant for hydroxyl−ether is indeed greater than the interassociations equilibrium constant of hydroxyl−carbonyl at room temperature. Table 2 lists all the parameters required by the Painter−Coleman association model[28] to estimate thermodynamic properties for this ternary phenolic/PEO/PCL blend.

Figure 2c shows infrared spectra of CH_2 wagging in the 1320−1380 cm^{-1} region of the pure PEO and various phenolic/PEO/PCL ternary blends. The pure PEO has two bands at 1360 and 1343 cm^{-1} that represent the crystalline phase of the PEO.[29] These crystalline bands disappear over the entire blends and are replaced by a broad band corresponding to the amorphous phase. The PEO crystallization is retarded and even inhibited by adding the phenolic resin component. As a result, we can confirm that this phenolic/PEO/PCL ternary blend series containing a constant 80 wt % of phenolic is totally miscible on the basis of the DSC and FTIR analyses. Furthermore, the interassociation equilibrium constant between hydroxyl−ether is greater than that of the interassociations equilibrium constant between hydroxyl−carbonyl at room temperature. On the other hand, the K_A values of phenolic−PEO and phenolic−PCL are both greater than the self-association equilibrium constant, indicating that the hydroxyl group of phenolic tends to form the interassociation than to form the self-association hydrogen bonding.

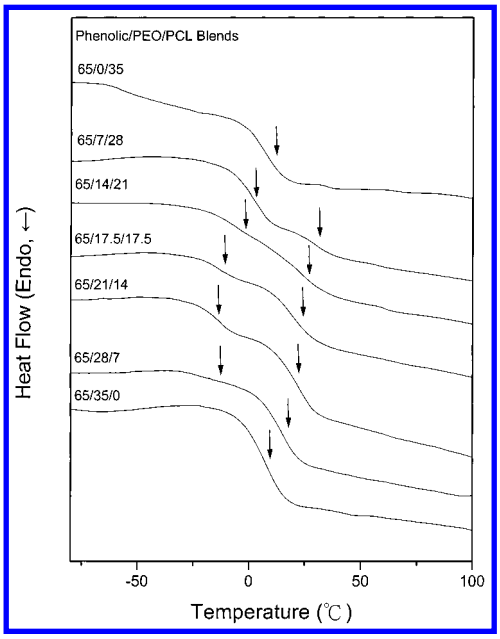

Figure 3. DSC thermograms of ternary blend of phenolic/PEO/PCL containing a constant composition (65 wt %) of phenolic resin.

Now, we turn our attention to those ternary blend containing lower (65 wt %) phenolic resin. Figure 3 shows the second run DSC thermograms of various phenolic/PEO/PCL ternary blends containing a fixed 65 wt % phenolic resin. The binary phenolic/PEO and phenolic/PCL blends show a single T_g, revealing that these binary blends are miscible in the amorphous phase. However, all these phenolic/PEO/PCL ternary blends containing 65 wt % phenolic have two T_g's, implying that they are immiscible in the amorphous phase. In general, the phase separation in a ternary blend is caused by the so-called $\Delta\chi$ effect, which is the difference in physical interaction between phenolic/PEO and phenolic/PCL. In addition, the difference in inter-

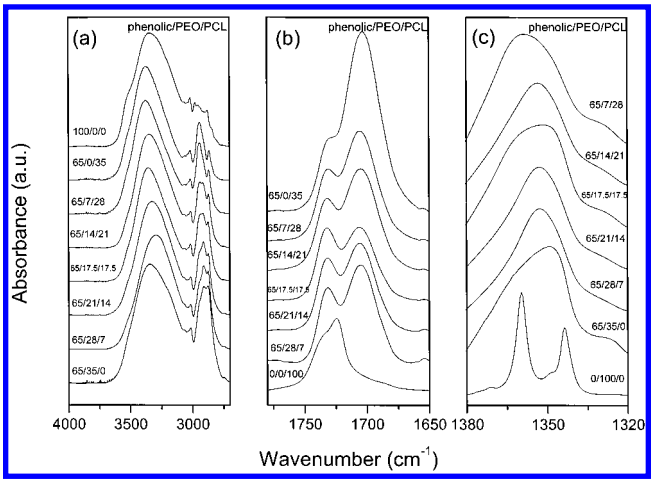

Figure 4. Infrared spectra of ternary blend of phenolic/PEO/PCL containing a constant composition (65 wt %) of phenolic resin at room temperature in the hydroxyl stretching region (a), carbonyl stretching region (b), and ether region (c).

association equilibrium constant also tends to induce phase separation. The phenolic is more favorable to interact with PEO than the PCL which is defined as the ΔK effect. By taking into account these two effects, it is difficult to find a ternary blend that is totally miscible over the entire compositions.[30] According to Table 2, the ΔK effect is significant because the interassociation equilibrium constant between phenolic hydroxyl group and PEO ether group is greater than the interassociation equilibrium constant between hydroxyl group of phenolic and carbonyl group of PCL. Therefore, these phenolic/PEO/PCL ternary blends containing a fixed phenolic content (65 wt %) have two T_g's. The higher and lower T_g are come from the phenolic−PEO and the phenolic−PCL phases because the interassociation equilibrium constant between phenolic hydroxyl group and PEO ether group is greater than the interassociation equilibrium constant between hydroxyl group of phenolic and carbonyl group of PCL. Figure 4 shows infrared spectra of these phenolic/PEO/PCL ternary blends containing a fixed phenolic content (65 wt %). The same trend in hydroxyl, carbonyl, ether vibration is observed as that shown in Figure 2. Fractions of hydrogen-bonded carbonyl group of the PCL are also summarized in Table 1. The K_A value calculated from eqs 5−9 based on the experimental fraction of hydrogen-bonded carbonyl group is $K_A = 325.6$ at room temperature, which is greater than that from the blend series containing 80 wt % phenolic. However, we consider that this K_A is unable to represent the true K_A because the phase separation occurs in this series of blends. Since the K_A value between phenolic hydroxyl group and PEO ether group is greater than the K_C value between phenolic hydroxyl group and PCL carbonyl group, the phenolic resin is more favorable to the PEO over the PCL. That means the K_A value will increase from the miscible ternary blend to the phase separation blend due to more intermolecular interaction between phenolic hydroxyl group and PEO ether group at beginning of phase separation stage. Interestingly, the fraction of hydrogen bonding decreases from 65/0/35 to 65/17.5/17.5, but it increases from 65/17.5/17.5 to 65/28/7 based on Table 1. This phenomenon is attributed to the fact that the relatively lower PCL content can form a greater fraction of hydrogen bonding at the 65/28/7 than 65/17.5/17.5 blend composition.

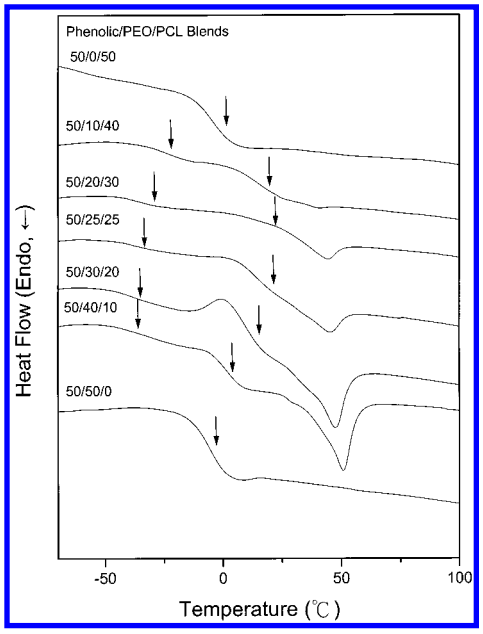

Figure 5. DSC thermograms of ternary blend of phenolic/PEO/PCL containing a constant composition (50 wt %) of phenolic resin.

Figure 5 shows the second run DSC thermograms of various phenolic/PEO/PCL ternary blends containing a constant phenolic content of 50 wt %. Again, these binary blends of phenolic−PEO and phenolic−PCL give a single T_g. These ternary blend of phenolic/PEO/PCL give two T_g's We need to point that the second T_g of phenolic/PEO/PCL = 50/30/20, 50/25/25, and 50/20/30 blend is overlapped with the exothermic crystallization peak. Interestingly, the melting temperature peak shifts to higher temperature with increasing the relative ratio of PEO to PCL. It is well-known that the melting temperatures of PEO (70 °C) and PCL (60 °C) are very close to each other. Initially, this melting temperature seems to come from the PEO with the increase of the PEO content. However, by taking into account the concept of competing equilibrium constants, the hydroxyl−ether interassociation equilibrium constant is greater than the hydroxyl−carbonyl interassociation equilibrium constant. The hydroxyl−carbonyl interassociation gradually breaks down with increasing PEO content in these ternary blends. As a result, the PCL will be excluded from the miscible system to form its own domain, and crystallization occurs. Figure 6 shows their corresponding infrared spectra at room temperature. The hydroxyl stretching containing a constant phenolic (50 wt %) (Figure 6a) shows the same trend as that shown in Figures 2a and 4a. The carbonyl stretching in Figure 6b reveals that the fraction of hydrogen-bonded carbonyl decreases with increasing the relative ratio of PEO to PCL, and the phenolic/PEO/PCL = 50/40/10 shows the crystalline conformations at 1724 cm^{-1}; the curve-fitting results are also summarized in Table 1. However, the CH_2 wagging of PEO in Figure 6c displays that the crystalline bands disappear and are replaced by a broad band roughly centered at 1350 cm^{-1} corresponding to the amorphous phase for all these ternary blends. However, the differences in crystallization behaviors are observed between DSC and FTIR analyses for phenolic/PEO/PCL = 50/30/20, 50/25/25, and 50/20/30 blend. In general, the polymer crystallinity measured by FTIR is from in-situ measurement, and no thermal history is involved in preparing the sample.

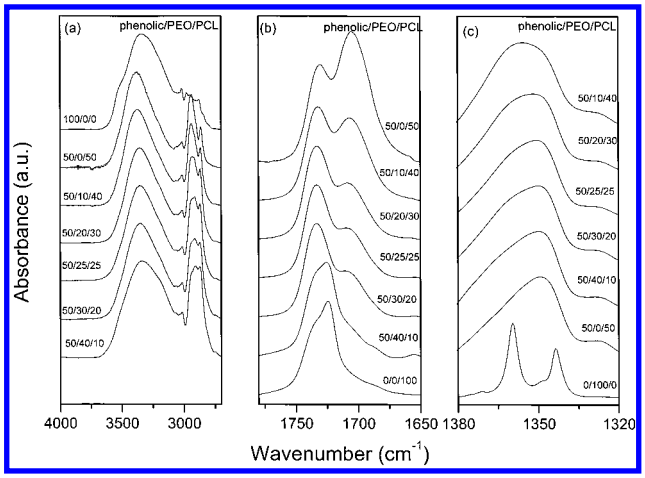

Figure 6. Infrared spectra of ternary blend of phenolic/PEO/PCL containing a constant composition (50 wt %) of phenolic resin at room temperature in the hydroxyl stretching region (a), carbonyl stretching region (b), and ether region (c).

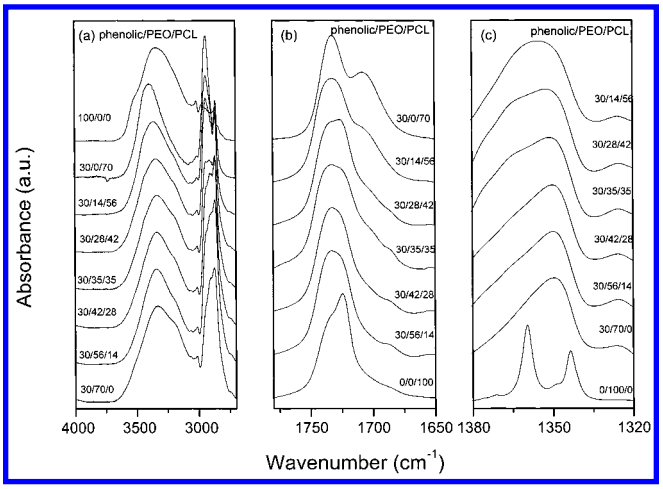

Figure 8. Infrared spectra of ternary blend of phenolic/PEO/PCL containing a constant composition (30 wt %) of phenolic resin at room temperature in the hydroxyl stretching region (a), carbonyl stretching region (b), and ether region (c).

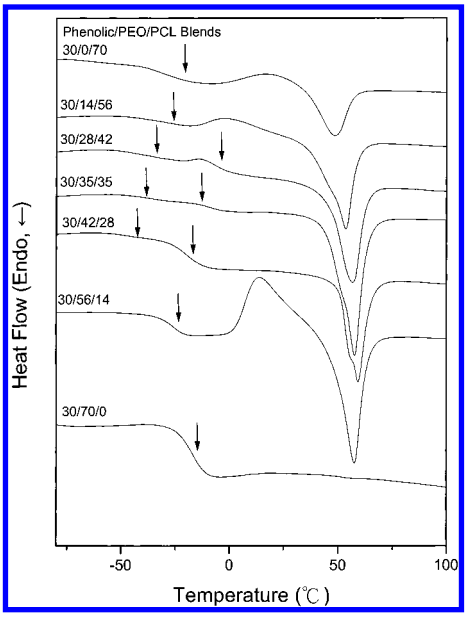

Figure 7. DSC thermograms of ternary blend of phenolic/PEO/PCL containing a constant composition (30 wt %) of phenolic resin.

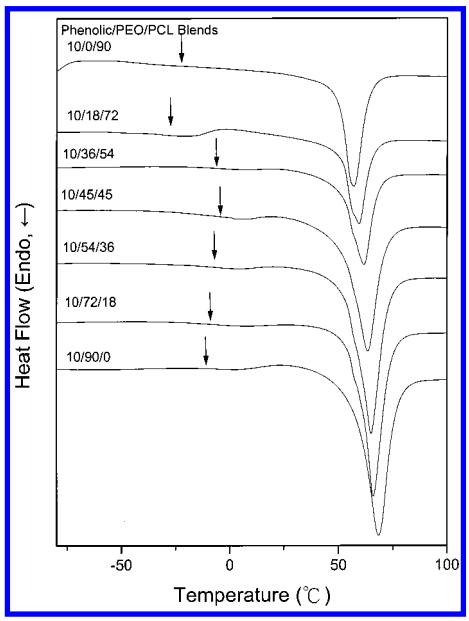

Figure 9. DSC thermograms of ternary blend of phenolic/PEO/PCL containing a constant composition (10 wt %) of phenolic resin.

On the contrary, the polymer crystallinity detected by DSC depends on the thermal history because recrystallization may occur during cooling or heating scan. Consequently, we are able to confirm that the melting temperature shown in Figure 5 is from the PCL, and the melting temperature shifting to higher temperature is due to the completing crystallization of PCL with increasing PEO content.

Figure 7 shows the second run DSC thermograms of phenolic/PEO/PCL ternary blends containing a constant 30 wt % of phenolic resin. Again, these binary blends, phenolic/PEO and phenolic/PCL, are miscible in the amorphous phase based on single detected by DSC. In addition, the ternary blend of phenolic/PEO/PCL = 30/56/14 and 30/14/56 shows one T_g because the phenolic is able to produce efficient intermolecular interaction with both PEO and PCL simultaneously. On the contrary, ternary blends of phenolic/PEO/PCL = 30/42/28, 30/35/35, and 30/28/42 shows two T_g's, indicating that these compositions are immiscible in the amorphous phase due to significant "$\Delta\chi$" and "ΔK" effects in these ternary polymer blends. Figure 8 shows their corresponding infrared spectra at room temperature, revealing that the melting temperature in Figure 7 has also come from the crystallization of PCL. Meanwhile, the free hydroxyl absorption of pure phenolic in Figure 8 decreases with increasing PEO and PCL content, indicating that the interassociation is present between phenolic and PEO or PCL in these ternary blends. This result is consistent with the observed higher interassociation equilibrium constants of phenolic/PEO, or phenolic/PCL is greater than the self-association equilibrium constant of the pure phenolic resin.

Figure 9 shows the second run DSC thermograms of the phenolic/PEO/PCL ternary blend containing a constant low phenolic content (10 wt %). Essentially all these ternary blends show one single glass transition temperature, indicating that these ternary blends are all miscible in the amorphous phase. It is well-known that the T_g cannot be detected for those high crystalline polymers. Figure 10 shows their corresponding infrared spectra at room temperature, revealing that the melting

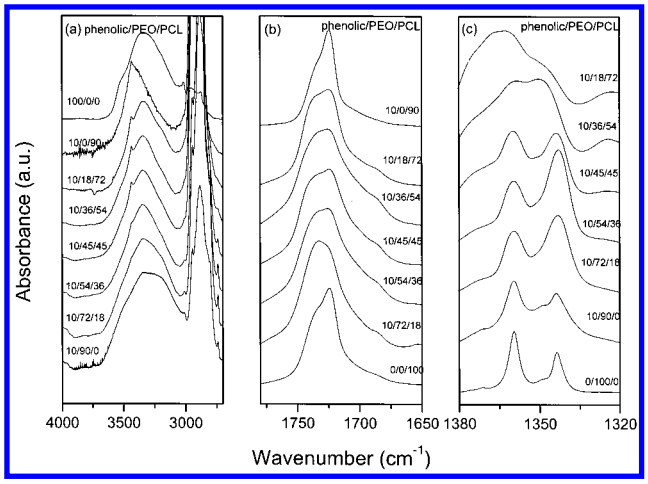

Figure 10. Infrared spectra of ternary blend of phenolic/PEO/PCL containing a constant composition (10 wt %) of phenolic resin at room temperature in the hydroxyl stretching region (a), carbonyl stretching region (b), and ether region (c).

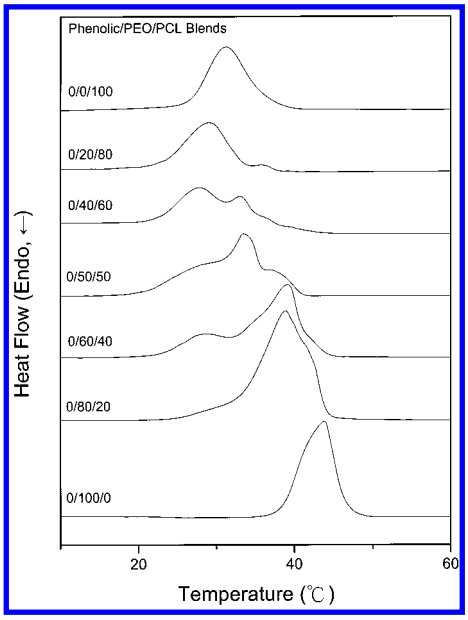

Figure 11. DSC thermograms of pure PEO, pure PCL, and their binary blends.

temperature in Figure 9 is come from the crystalline of PEO and PCL. For those ternary blends, phenolic/PEO/PCL = 10/18/72 and 10/36/54, the crystalline bands disappear the crystallization of PEO because the crystalline bands are replaced by a broad band roughly centered at 1350 cm^{-1} corresponding to the amorphous phase. It is reasonable that lower PEO content in the blend is able to for more perfect interassociation interaction between phenolic and PEO segment.

Finally, there exists an important problem of whether the binary blend of PEO/PCL is miscible or immiscible in the amorphous phase. Since the glass transition temperatures of PEO and PCL are very close and the miscibility between PEO and PCL is unable to be determined by using one or two T_g. Figure 11 shows the DSC thermogram of pure PEO, PCL and various PEO/PCL binary blend by using a slow cooling rate (5 °C/min) to determine the crystallization temperature. Fortunately, the crystallization temperatures of PEO/PCL binary blend are depressed with their respective homopolymer. This result reveals that the PEO or PCL chains are able to penetrate and to insert into the

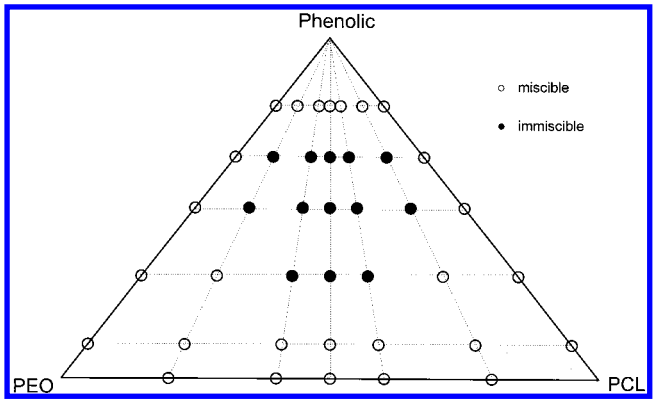

Figure 12. Ternary phase diagram of the phenolic/PEO/PCL system. The open circles represent a miscible ternary blend, and the full circles represent an immiscible ternary blend.

lamella region of other homopolymers. Therefore, we can consider that this binary blend of PEO/PCL is miscible in their amorphous phase such as PBA/PEO, PVDF/PBA, and PVPF/PBSU blend systems.[31,32] The phase diagram of this ternary phenolic/PEO/PCL blend at room temperature is present in Figure 12 based on DSC analyses. There exists a closed-looped of phase separated region in the phase diagram due to the so-called "$\Delta\chi$" and "ΔK" effects in ternary polymer blends. The phase behavior can be theoretically predicted and compared with the experimental data. The exact calculation of the phase diagram is difficult due to no analytical expression for the binodal curve. In general, the spinodal based on the Flory−Huggins lattice theory has been used to reproduce the experimental boundary. The free energy of mixing per unit volume of three monodisperse homopolymers is given by[33]

$$\frac{\Delta G_m}{V} = RT\left(\frac{\phi_1 \ln \phi_1}{V_1} + \frac{\phi_2 \ln \phi_2}{V_2} + \frac{\phi_3 \ln \phi_3}{V_3}\right) + B_{12}\phi_1\phi_2 + B_{13}\phi_1\phi_3 + B_{23}\phi_2\phi_3 \quad (10)$$

where V is the mixture volume, V_i is the molar volume of component i, and B_{ij} is the Flory interaction energy density between segments of polymer i and j. The B_{ij} value can be experimentally determined by several techniques such as solubility difference, small-angle neutron scattering, melting temperature depression, vapor sorption, analogue calorimetry, and copolymer phase behavior.[34] The boundary condition for the spinodal curve is given by the following condition:[35]

$$\left[\frac{\partial^2(\Delta G_m/V)}{\partial \phi_1{}^2}\right]_{T,P}\left[\frac{\partial^2(\Delta G_m/V)}{\partial \phi_2{}^2}\right]_{T,P} - \left[\frac{\partial^2(\Delta G_m/V)}{\partial \phi_1\, \partial \phi_2}\right]^2 = 0 \quad (11)$$

From eqs 10 and 11, the equation for the spinodal of a ternary polymer blend is given explicitly by[36−38]

$$\left(\frac{RT/V_1}{\phi_1} + \frac{RT/V_3}{\phi_3} - 2B_{13}\right)\left(\frac{RT/V_2}{\phi_2} + \frac{RT/V_3}{\phi_3} - 2B_{23}\right) - \left(\frac{RT/V_3}{\phi_3} + B_{12} - B_{13} - B_{23}\right)^2 = 0 \quad (12)$$

We must know the B_{ij} value for each of the binary blends in this system to compare the experimental data with theoretical prediction. The values of $B_{\text{phenolic/PCL}} = -12.51$ and $B_{\text{phenolic/PEO}} = -2.48$ cal/cm^3 have been

determined in our previous study[39] and Sotele et al.[40] by using melting temperature depression based on the Nishi−Wang equation.[41] The value of $B_{PEO/PCL}$ is obtained by using various values predicted from the phase diagram based on eq 12. The $B_{PEO/PCL}$ value of −2.85 cal/cm^3 gives the best fit by the predicted spinodal. The negative value of $B_{PEO/PCL}$ indicates that the binary blend of PEO/PCL is miscible in the amorphous phase, and this result is consistent with the previous DSC analyses.

Conclusions

The phase behavior and hydrogen bonding of ternary blend of phenolic/PEO/PCL have been investigated by using DSC and FTIR analyses. Although all three individual binary blends are miscible in the amorphous phase, there still exists a close-loop immiscibility region in the phase diagram due to the significant "$\Delta\chi$" and "ΔK" effects in ternary polymer blends. The interassociation equilibrium constant between hydroxyl group of phenolic and ether group of PEO is determined indirectly from a least-squares fitting procedure based on the experimental fraction of hydrogen-bonded carbonyl group in this ternary polymer blend system by taking into account the intramolecular screening and functional group accessibility effects. The observed K_A (264.7) of hydroxyl−ether is found substantially higher than the K_C = 116.8 from the hydroxyl−carbonyl formation and the K_B = 52.3 from the hydroxyl multimer formation. This result implies that the tendency toward forming the hydrogen bonding between phenolic and PEO dominates over the interassociation of the phenolic with PCL and the self-association by forming the intramolecular hydrogen bonding of the pure phenolic resin. The theoretical prediction based on the Flory−Huggins lattice theory was compared with the experimental data, and the value of $B_{PEO/PCL}$ was obtained to be −2.85 cal/cm^3, indicating that the binary blend of PEO/PCL is miscible in the amorphous phase.

Acknowledgment. The authors thank the National Science Council, Taiwan, Republic of China, for financially supporting this research under Contract NSC-90-2216-E-009-026.

References and Notes

(1) Winey, K. I.; Berba, M. L.; Galvin, M. E. *Macromolecules* **1996**, *29*, 2868.
(2) Hong, B. K.; Kim, J. K. Jo, W. H.; Lee, S. C. *Polymer* **1997**, *38*, 4373.
(3) Manestrel, C. L.; Bhagwagar, D. E.; Painter, P. C.; Coleman, M. M.; Graf, J. F. *Macromolecules* **1992**, *25*, 7101.
(4) Jo, W. H.; Kwon, Y. K.; Kwon, I. H. *Macromolecules* **1991**, *24*, 4708.
(5) Pomposo, J. A.; Calahorra, E.; Eguiazabal, I.; Cortazar, M. *Macromolecules* **1993**, *26*, 2104.
(6) Zhang, H.; Bhagwagar, D. E.; Graf, J. F.; Painter, P. C.; Coleman, M. M. *Polymer* **1994**, *35*, 5379.
(7) Chiang, C. R.; Chang, F. C. *J. Polym. Sci., Part B* **1998**, *36*, 1085.
(8) Ju, M. Y.; Chang, F. C. *Polymer* **2000**, *41*, 2000.
(9) Tseng, F. P.; Lin, J. J.; Tseng, C. R.; Chang, F. C. *Polymer* **2001**, *42*, 713.
(10) Kuo, S. W.; Chang, F. C. *Macromol. Chem. Phys.* **2001**, *202*, 3112.
(11) Wu, H. D.; Chu, P. P.; Ma, C. C. M.; Chang, F. C. *Macromolecules* **1999**, *32*, 3097.
(12) Etxeberria, A.; Guezala, S.; Iruin, J. J.; Campa, J. G.; Abajo, J. D. *Polymer* **1998**, *39*, 1035.
(13) Mekhilef, N.; Hadjiandreou, P. *Polymer* **1995**, *36*, 2165.
(14) Qin, C.; Pires, A. T. N.; Belfiore, L. A. *Macromolecules* **1991**, *24*, 666.
(15) Coleman, M. M.; Yang, X.; Painter, P. C.; Graf, J. F. *Macromolecules* **1992**, *25*, 4414.
(16) Chu, P. P.; Wu, H. D.; Lee, C. T. *J. Polym. Sci., Part B* **1998**, *36*, 1647.
(17) Coggesthall, N. D.; Saier, E. L. *J. Am. Chem. Soc.* **1951**, *71*, 5414.
(18) Painter, P. C.; Veytsman, B.; Kumar, S.; Shenoy, S.; Graf, J. F.; Xu, Y.; Coleman, M. M. *Macromolecules* **1997**, *30*, 932.
(19) Coleman, M. M.; Pehlert, G. J.; Painter, P. C. *Macromolecules* **1996**, *29*, 6820.
(20) Pehlert, G. J.; Painter, P. C.; Veytsman, B.; Coleman, M. M. *Macromolecules* **1997**, *30*, 3671.
(21) Pehlert, G. J.; Painter, P. C.; Coleman, M. M. *Macromolecules* **1998**, *31*, 8423.
(22) Coleman, M. M.; Guigley, K. S.; Painter, P. C. *Macromol. Chem. Phys.* **1999**, *200*, 1167.
(23) Painter, P. C.; Coleman, M. M. In *Polymer Blends*; Paul, D. R., Ed.; John Wiley & Sons: New York, 2000; Vol. 1.
(24) Wu, H. D.; Ma C. C. M.; Chu P. P. *Polymer* **1997**, *38*, 5419.
(25) Moskala, E. J.; Varnell, D. F.; Coleman, M. M. *Polymer* **1985**, *26*, 228.
(26) Kuo, S. W.; Chang, F. C. *Polymer* **2001**, *42*, 9843.
(27) Kuo, S. W.; Chang, F. C. *Macromolecules* **2001**, *34*, 4089.
(28) Coleman, M. M.; Graf, J. F.; Painter, P. C. *Specific Interactions and the Miscibility of Polymer Blends*; Technomic Publishing: Lancaster, PA, 1991.
(29) Chintapalli, S.; Frech, R. *Macromolecules* **1996**, *29*, 3499.
(30) Coleman, M. M.; Painter, P. C. *Prog. Polym. Sci.* **1995**, *20*, 1.
(31) Liu, A. S.; Liau, W. B.; Chiu, W. Y. *Macromolecules* **1998**, *31*, 6593.
(32) Chen, H. L.; Wang, S. F. *Polymer* **2000**, *41*, 5157.
(33) Flory, P. J. *Principles of Polymer Chemistry*; Cornell University Press: Ithaca, NY, 1953.
(34) Merfeld, G. D.; Paul, D. R. In *Polymer Blends*; Paul, D. R., Ed.; John Wiley & Sons: New York, 2000; Vol. 1.
(35) Su, A. C.; Fried, J. R. *Polym. Eng. Sci.* **1987**, *27*, 1657.
(36) Kim, C. K.; Paul, D. R. *Macromolecules* **1992**, *25*, 3097.
(37) Scott, R. L. *J. Chem. Phys.* **1949**, *17*, 279.
(38) Zeman, L.; Patterson, D. *Macromolecules* **1972**, *5*, 513.
(39) Kuo, S. W.; Huang, C. F.; Chang, F. C., *J. Polym. Sci., Polym. Phys. Ed.* **2001**, *39*, 1348.
(40) Sotele, J. J.; Soldi, V.; Pires, A. T. N. *Polymer* **1997**, *38*, 1179.
(41) Nishi, T.; Wang, T. T. *Macromolecules* **1975,** *8*, 909.

MA011255F